

Confusing dark matter particle properties with modifications to General Relativity

Armando A. Roque¹ and J. Barranco¹

¹*Division de Ciencias e Ingenierías, Universidad de Guanajuato,
Campus Leon, C.P. 37150, León, Guanajuato, México.*

(Dated: April 5, 2022)

Cold Dark Stars made of self-gravitating fermions in the degenerate limit are constructed in General Relativity and in R-square gravity, $f(R) = R + \alpha R^2$. The properties of the resulting Cold Dark Stars in both theories of gravity are studied. It is found that the same gravitational potential is generated for different election of the parameters of the model, such as the mass of the fermion, the self-interacting strength or the value of α , thus, a possible confusion in the determination of the dark matter properties and the favored theory of gravity might arise.

I. INTRODUCTION

Current astrophysical observations favor General Relativity (GR) as the correct theory that describes the gravitational interaction [1, 2]. Nevertheless, if GR is valid, in order to have a concordance model for the evolution of the universe, two dark components must be added to the energy density content of the universe i.e. Dark Matter (DM) and Dark Energy (DE), the latest in the form of a cosmological constant. This model that have as main ingredients GR, DM as a cold heavy non relativistic particle and a cosmological constant is known as the Λ -CDM model [3]. This model is consistent with most of the observational data (e.g. measurement of anisotropies in the temperature and polarization of the cosmic microwave background (CMB) [4], fluctuations in the density of baryonic matter (BAO) [5–7], observations of the magnitude-redshift relation for high redshift SNe Ia [8, 9]) among many other observations. However, there are some unresolved problems: the Planck best-fit measurements of the current expansion rate H_0 [10] is in tension with the value obtained by local measurements of H_0 [11–14]. Furthermore, the Λ -CDM model is not compatible with some astrophysical observations at galactic scales. Perhaps more important, Λ -CDM model has little to say about the nature of dark matter, except that it could be a heavy neutral particle that interacts very weakly with the rest of the particles of the Standard Model of particle physics (SM).

An unpleasant possibility, although favored by its simplicity, is that DM particles interact only through gravitational interactions, and thus, the only parameters to be determined are the spin and the mass of the dark matter particle, plus the coupling constants that parametrize the interactions among themselves.

If DM has no other interaction than gravitational, then DM particle properties will be obtained only through astrophysical observations of the dynamics of visible objects with the gravitational force generated by the DM.

In this scenario, another unpleasant possibility is that *there is a degeneracy in the determination of the DM properties once variations to the theory of General Relativity are allowed*. The objective of this work is to show one example of this possibility.

For definitiveness, we will consider as a model for DM particles, fermions of mass m that have not any other interaction with the standard model of particles except the gravitational interaction. In particular this model of fermionic dark matter has been used to model dark matter halos [15–21]. This dark matter fermions can interact themselves and thus a self-interaction term will be added [22].

On the other hand, as for modification of GR, we will focus on a theory of gravity that is derived from the action

$$S = - \int d^4x \sqrt{-g} (R + \alpha R^2), \quad (1)$$

where R is the Ricci scalar. This is known as R-square gravity or as the Starobinsky model [23–25]. This modification to GR is a particular case of the so-called $f(R)$ theories of gravity [26]. Note that R-square gravity is not introduced to solve the low energy problems of GR such as to avoid the introduction of dark matter or dark energy. Instead, we have used it because R-square gravity it is the simplest non trivial four-derivative extension of GR that is free of ghosts [25, 26] and thus it is a natural extension to GR to be studied. We have been motivated to use this fermionic dark matter model and R-square gravity because the minimal number of parameters that are introduced. Even in this minimal scenario we will show there could be a confusion in the determination of fermions properties for different values of α . In general, other modifications to GR have more than one free parameter, thus strengthening the confusing of DM properties. (e.g. Hu & Sawicki model [27], Starobinsky (2007) [28], The exponential model [29, 30]).

For a distant observed, the gravitational effects of compact objects depend only of their total mass and radius (i.e. the compactness). What we will show is that self-gravitating configurations made of DM fermions will have the same mass and radius although in one case one configuration is made of fermions with a specific value of self-interacting coupling constant in General relativity while the equivalent configuration is made for a different self-interacting constant but in R-square gravity. Thus, there is a possible confusion in the determination of the dark matter properties. Even in this very simplified scenario

where few parameters are present. In the case where DM-SM interactions are introduced, a bigger indetermination will be expected.

Next, we solve the Tolman-Oppenheimer-Volkov equations in order to find the self-gravitating configurations made of this self-interacting fermions in both GR and R-square theories of gravity. We will call this DM self-gravitating compact objects as Cold Dark Stars (CDS). We study the general properties of CDS and we will find equivalent configurations for different elections of parameters.

The paper is organized as follows: In Section II we obtain the self-gravitating objects made of fermionic dark matter (CDS) both in General Relativity and in R-square gravity. Some previous results in GR are reproduced [31] and new results are obtained, specially those concerning the compactness of the resulting configurations. We present in section III a comparison of CDS in GR and R-square gravity and the equivalence of some configurations even for different values of the self-interacting coupling, i.e. a confusion on the determination of the DM properties. In Section IV we give some concluding remarks.

II. COLD DARK STARS

Dark matter over-densities might form small clumps that can evolve into Dark Stars, i.e self-gravitating objects made of dark matter [32–34]. It is generally assumed that those Dark Stars will be powered by the heat from dark matter annihilation, rather than by fusion. In our case, since we are assuming that DM has no interaction with SM particles, thus, our Dark Stars will be Cold compact objects and in order to distinguish from dark stars we will call the resulting self-gravitating objects made of Fermionic DM in the degenerate limit as Cold Dark Stars.

A. CDS in General Relativity

For non interacting fermions in the degenerate limit, it is possible to establish a relationship between the pressure and the density, for a gas of free fermions. This relationship can be calculated via explicit expressions for the energy density ρ and pressure p . For a completely degenerate gas of fermions ρ and p are given by [31, 35] (in units where $c = \hbar = 1$):

$$\rho(z) = \frac{m^4}{8\pi^2} \left[(2z^3 - 3z) (1 + z^2)^{1/2} + 3 \sinh^{-1}(z) \right], \quad (2)$$

$$p(z) = \frac{m^4}{24\pi^2} \left[(2z^3 + z) (1 + z^2)^{1/2} - \sinh^{-1}(z) \right], \quad (3)$$

where $z = k_f/m$ is the dimensionless Fermi momentum and m the mass of the fermion. It is convenient to work

in dimensionless variables so we define the dimensionless variables

$$\bar{p} = \frac{p}{m^4}, \quad \bar{\rho} = \frac{\rho}{m^4}, \quad \bar{r} = r \frac{m^2}{m_p}, \quad (4)$$

where, m is the fermion mass, and m_p is the Planck mass, defined as $m_p = G^{-1/2}$.

We will consider self-interacting dark matter since it may resolve some problems of Λ -CDM paradigm at galactic scales [36]. Following [31], the interparticle interactions can be added effectively by adding a term proportional to the square of the density number of fermions:

$$\bar{\rho}(z) = \frac{1}{8\pi^2} \left[(2z^3 - 3z) (1 + z^2)^{1/2} + 3 \sinh^{-1}(z) \right] + \frac{1}{9\pi^4} y^2 z^6. \quad (5)$$

$$\bar{p}(z) = \frac{1}{24\pi^2} \left[(2z^3 + z) (1 + z^2)^{1/2} - \sinh^{-1}(z) \right] + \frac{1}{9\pi^4} y^2 z^6, \quad (6)$$

where y is the interaction strength between fermions.

In order to obtain the self-gravitating object made of this gas of fermions, it is needed to solve Einstein's equations and the conservation of the energy tensor.

Taking $\alpha = 0$ in eq. (1), the action reduces to the General Relativity action. We consider a static, spherically symmetric ansatz for the line element,

$$ds^2 = -A^2(r)dt^2 + B^2(r)dr^2 + r^2 d\theta^2 + r^2 \sin^2 \theta d\varphi^2. \quad (7)$$

The energy momentum tensor for a perfect fluid is given by

$$T^{\mu\nu} = (\rho + p)u^\mu u^\nu + g^{\mu\nu}p \quad (8)$$

and thus, Einstein-equations reduces to the Tolman-Oppenheimer-Volkoff equations (TOV):

$$B' = \frac{B^3 (8\pi \bar{r}^2 \bar{\rho} - 1) + B}{2\bar{r}}, \quad (9)$$

$$2A' = \frac{A (B^2 (8\pi \bar{r}^2 \bar{p} + 1) - 1)}{\bar{r}}, \quad (10)$$

$$\bar{p}' = -\frac{A'(\bar{\rho} + \bar{p})}{A}, \quad (11)$$

We set as boundary conditions $A(0) = B(0) = 1$, $\bar{p}(0) = \bar{p}_0$, with \bar{p}_0 a free parameter. As the equation of state depends on two parameters, z and y , the $\bar{\rho}(\bar{p})$ relationship was obtained of interpolation of results of evaluate eq. (5) and eq. (6) for a range of values $0 < z < 20$ given a fixed interaction strength y . The range of values explored for y are between 0 and 10. And, for our analysis, the central pressure of the object \bar{p}_0 , took values between 10^{-10} to 10. The mass of this objects was cal-

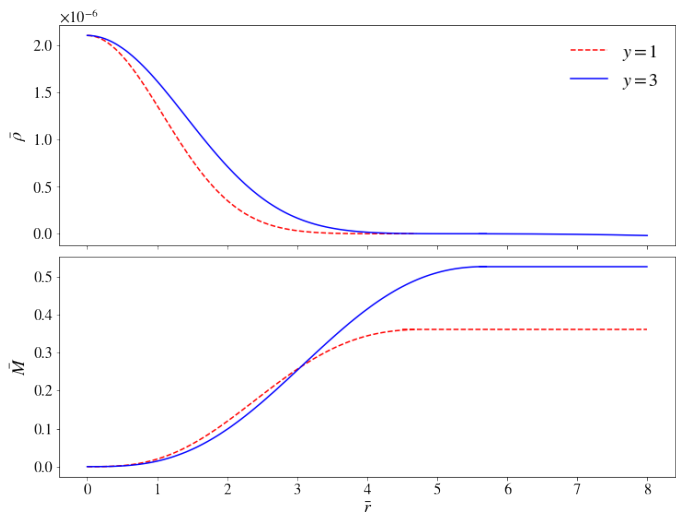


FIG. 1: Typical energy density profile and mass as a function of the radial coordinate r . For definitiveness it was chosen $\bar{\rho}_0 = 2.1 \times 10^{-6}$, and two values of the self-interacting strength: $y = 1$ (dashed line) and $y = 3$ (solid line). The introduction of self-interaction produces a more massive self-gravitating structure and with a stiffer density profile.

culated using the ADM mass,

$$M_{\text{ADM}} = \frac{1}{2} \bar{r} \left(1 - \frac{1}{B^2} \right). \quad (12)$$

Typical configurations are shown in Fig. 1, where the profile for the energy density as a function of \bar{r} are shown for a fixed value of $\bar{\rho}_0$ (that is equivalent to a fixed value of $\bar{\rho}_0$) for two different values of the self-interacting strength y . For definitiveness it was chosen $\bar{\rho}_0 = 2.1 \times 10^{-6}$, and two values of the self-interacting strength: $y = 1$ (dashed line) and $y = 3$ (solid line). The introduction of self-interaction produces a more massive self-gravitating structure and with a stiffer density profile. The radius \bar{R} is defined as the point where the ADM Mass starts to be constant ($\bar{\rho} < 0$). Thus, each CDS will have a fixed total mass \bar{M} and a finite radius \bar{R} .

It is possible to obtain the full set of CDS for our parameter space $(\bar{\rho}_0, y) \rightarrow (\bar{R}, \bar{M}, y)$. These configurations are shown in Fig. 2. Note that, each value of y imply a different equation of state. For small values of this and lower densities, the interaction terms can be ignored and the object was describe for an ideal Fermi gas. For higher y values, the interaction terms become more and more important and the *transition point* from the relativistic curve to no relativistic move to lower densities. Similar behavior occur with the stability border of the dark star (we can defined the stability border from the maximum gravitational mass of the Cold Dark Star). It can be seen that the stability border move to right (lower central pressure) when is increasing the interaction strength parameter. As was expect, the mass ground for higher values of y , it is because the degeneration pressure is

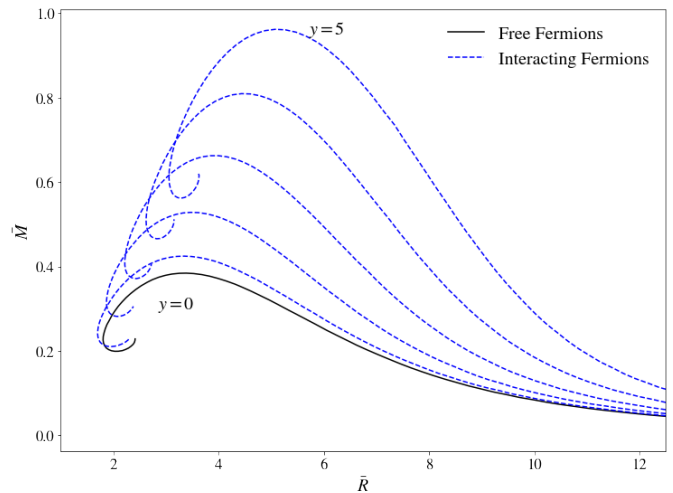


FIG. 2: Black solid line correspond to \bar{M} vs \bar{R} for $y = 0$ (General Relativity without auto-interaction) and the blues dotted-lines corresponds to the dark star made of interacting fermions in General Relativity with coupling constant for a rang between $y = 1$ and $y = 5$.

strengthened and it necessary more mass for counteract this, and arrived to hydrostatic equilibrium.

Because the dimensionless definitions of the variables eq. (4), all values obtained in Figs. 1-2 are dimensionless as well. In order to obtain the physical values of the mass and energy density we have the following relations

$$M_{\text{phys}} = \bar{M}_{\text{ADM}} \frac{m_p^3}{m^2}, \quad \rho_{\text{phys}} = \bar{\rho} m^4, \quad R_{\text{phys}} = \bar{R} \frac{m_p}{m^2}, \quad (13)$$

Note that if $m = 1$ KeV then $M_{\text{phys}} \sim 10^{12} M_\odot$ and $R_{\text{phys}} \sim 0.1 \text{ pc}$, e.g. a possible super massive black hole mimicker.

We finish this section by enumerating some general properties of CDS. In GR the self gravitating configurations made of degenerate non interacting fermions (CDS) have the following properties:

1. The total mass of the CDS increases as $\bar{\rho}_0$ increases, then the mass reaches a maximum value \bar{M}_{max} that defines the stability region.
2. The radius of the configuration \bar{R} decreases as $\bar{\rho}_0$ increases.
3. The introduction of a self-interacting coupling between the fermions ($y > 0$) make that the configuration increases the value of the maximum mass \bar{M}_{max}

B. Cold Dark Star in R square gravity

Now we study CDS in the R-square gravity given by the action eq. (1).

The generic field equations for a theory $f(R)$ are given by,

$$f_R R_{\mu\nu} - \frac{1}{2} g_{\mu\nu} f(R) + g_{\mu\nu} \square f_R - \nabla_\nu \nabla_\mu f_R = k T_{\mu\nu}, \quad (14)$$

where, $f_R := \partial_R f(R)$, $\square = g^{\mu\nu} \nabla_\mu \nabla_\nu$.

Taking $f(R) = R + \alpha R^2$, (where α is a constant with

units of the inverse of the Ricci scalar $[R^{-1}]$) in eq. (14) and using the 1-1, 2-2 components, and a spherically symmetric line element eq. (7) and the conservation equation $\nabla_\mu T^{\mu\nu} = 0$ with $T^{\mu\nu}$ a perfect fluid as before, it is possible to obtain the modified Tolman-Oppenheimer-Volkoff for R-square gravity. The R-square TOV system is given by:

$$B' = \frac{B \left(2 + B^2 (-2 + \bar{\alpha} \bar{R} (-4 + \bar{r}^2 \bar{R}) + 16\pi \bar{r}^2 \bar{\rho}) + 4\bar{\alpha} (\bar{R} + \bar{r} (2\bar{R}' + \bar{r} \bar{R}'')) \right)}{4\bar{r} (1 + 2\bar{\alpha} \bar{R} + \bar{r} \bar{\alpha} \bar{R}')} \quad (15)$$

$$A' = \frac{A \left(-2 - 4\bar{\alpha} \bar{R} + B^2 (2 + 16\pi \bar{r}^2 \bar{\rho} + \bar{\alpha} \bar{R} (4 - \bar{r}^2 \bar{R})) - 8\bar{r} \bar{\alpha} \bar{R}' \right)}{4\bar{r} (1 + 2\bar{\alpha} \bar{R} + \bar{r} \bar{\alpha} \bar{R}')} \quad (16)$$

$$\bar{p}' = -\frac{A'(\bar{\rho} + \bar{p})}{A} \quad (17)$$

For this case, we need a extra equation for describe the Ricci scalar behaviour because the theory have a extra

degree of freedom. It is given by:

$$\bar{R}'' = \frac{6\bar{\alpha} \bar{R}' (-1 - 2\bar{\alpha} \bar{R} + 2\bar{r} \bar{\alpha} \bar{R}') + B^2 (\bar{r} (1 + 2\bar{\alpha} \bar{R}) (24\pi \bar{p} + \bar{R} - 8\pi \bar{\rho}) + \bar{\alpha} (-6 + \bar{R} (\bar{r}^2 - 12\bar{\alpha} + 3\bar{r}^2 \bar{\alpha} \bar{R}) + 16\pi \bar{r}^2 \bar{\rho}) \bar{R}')}{6\bar{r} \bar{\alpha} (1 + 2\bar{\alpha} \bar{R})} \quad (18)$$

Note that eqs. (17)-(18) are written in dimensionless variables where we have used the extra variable change, $\alpha = \bar{\alpha} m_p^2 / m^4$ and $R = \bar{R} m^4 / m_p^2$.

The value of the free parameter α of R-squared theory is constrained from observations in different scales. In the cosmological context, if one takes $\alpha < 0$ then ghost modes instabilities arises [37]. Furthermore, for negative values of α , the Ricci scalar profile has a oscillating behaviour outside the star and this oscillating behaviour is in contradiction with our boundary conditions. Similar behaviour occurs in the neutron star context [38]. Then, we will work with $\alpha > 0$ values.

From the strong gravity regime, $|\alpha|$ is constrained to be $\lesssim 10^{10} \text{ cm}^2$ [39]. For weak-field limit, it is constrained by different experiments, the Eöt-Wash provides the more stringent bound, $|\alpha| \lesssim 10^{-6} \text{ cm}^2$, the Gravity Probe B, constrains $|\alpha|$ to have values $\lesssim 5 \times 10^{15} \text{ cm}^2$ and from measurements of the precession of the pulsar B in the PSR J0737-3039, $|\alpha| \lesssim 2.3 \times 10^{19} \text{ cm}^2$. [40] Although all the bounds has differences, they are still meaningful, because this type of theory present a chameleon effect and thus the α values could be different at different scales.

In our case, to compare α with $\bar{\alpha}$ we recall that

$$\alpha = 5.79 \times 10^{-5} \bar{\alpha} \left(\frac{m}{1 \text{ TeV}} \right)^{-2} \text{ cm}^2. \quad (19)$$

For $m \sim 1 \text{ TeV}$, values of $\bar{\alpha} \sim 10^{-1}$ will be in concordance with the strongest limit of $|\alpha| \lesssim 10^{-6} \text{ cm}^2$. We will find the configurations for a specific value of $\bar{\alpha} = 0.05$

The next step for the numerical analysis is to define the boundary conditions compatible with solutions that are regular at the origin, localized, and asymptotically flat. We expand the system equation around to the origin in order to find the boundary conditions at $r = 0$. It was found:

$$\bar{R}(0) = R_0, \quad \bar{R}'(0) = 0. \quad (20)$$

where the “prime” indicate derivation with respect to \bar{r} . Here R_0 has to be chosen so that the Ricci scalar vanishes asymptotically (at $r \rightarrow \infty$). The correct value of R_0 such as the boundary conditions are fulfilled is found with a shooting algorithm. [41]

Since R approaches asymptotically to zero, numerically we have to choose a particular value of r such that

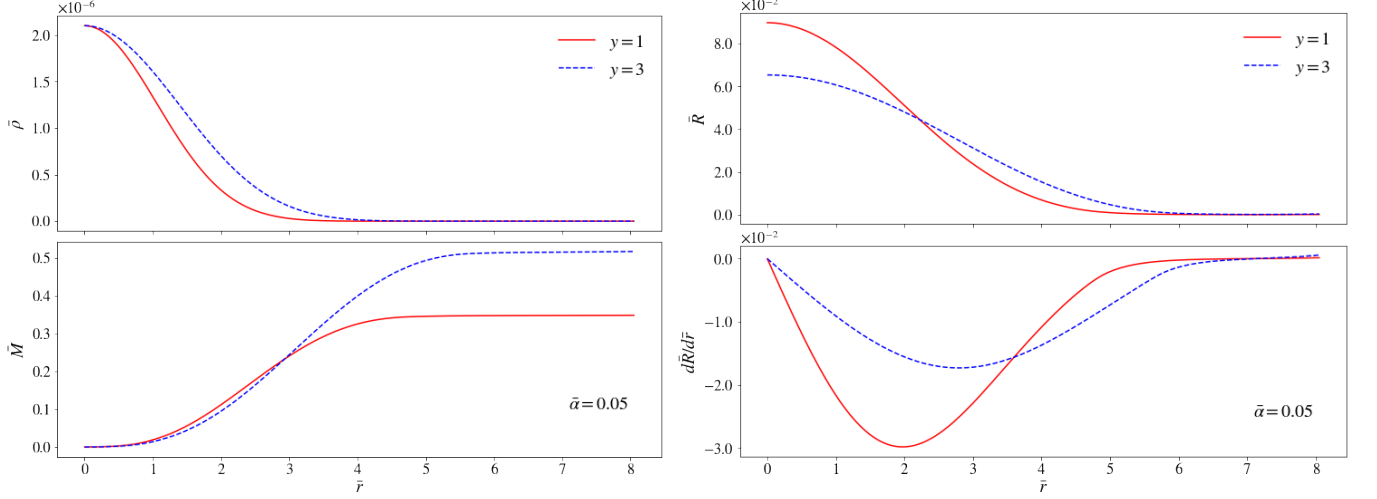


FIG. 3: Left panel: CDS density and Mass profile in R-square gravity with $\bar{\alpha} = 0.05$. As in Fig. 1, $\bar{\rho}_0 = 2.1 \times 10^{-6}$ and we have selected the values of the interaction strength $y = 1$ and $y = 3$. Right panel: The value of Ricci scalar in the origin was chosen so that asymptotically tend to zero.

the value of Ricci scalar is almost zero. Numerically we choose a value $\bar{r} = r_*$ such as $\bar{R}(r_*) \leq R_0/10^4$.

Because the Ricci scalar vanishes at infinity, the space-time metric approaches to the Schwarzschild space time and thus we can use the Schwarzschild metric to estimate the mass of object using (12) with $\bar{r} = r_*$. As the Ricci scalar does not strictly vanish for r_* , we demand that $\bar{M}'(r_*) \approx 0$ must be satisfied, the “prime” indicate derivation respect to \bar{r} .

The system equations (15)-(18) were solved numerically with an equation of state given as in the previous section, i.e. a equation of state for a gas of self-interacting fermions in the degenerate limit. Typical selfgravitating configurations for two different values of the coupling strength ($y = 1$ red solid line and $y = 3$ blue line) are shown in Fig. 3. It is shown the density, $\bar{\rho}(\bar{r})$, and mass, $\bar{M}(\bar{r})$, profiles for the specific value of the central pressure $\bar{\rho}_0 = 2.1 \times 10^{-6}$. The profile for the Ricci scalar and their derivative are also shown in Fig. 3.

We finish this section by constructing all configurations for a specific value of $\bar{\alpha} = 0.05$. Solutions in the \bar{M} vs \bar{R} space for different values of the self-interacting strength y are shown in Fig. 4.

In R-square gravity the CDS have the same behaviour as in GR, but the new parameter $\bar{\alpha}$ modifies the global structure of the configuration. In particular, in R-square gravity the maximum masses \bar{M}_{max} are smaller than the GR case for the same value of the self-interacting coupling constant y (see Figs. 2-4). In order to understand this behaviour, let us take the Newtonian limit of R-square gravity.

In this case, the Newtonian gravitational potential for R-square gravity is [42]:

$$V(r) = -\frac{GM}{r} - \frac{GM}{3r}e^{-\beta r}, \quad (21)$$

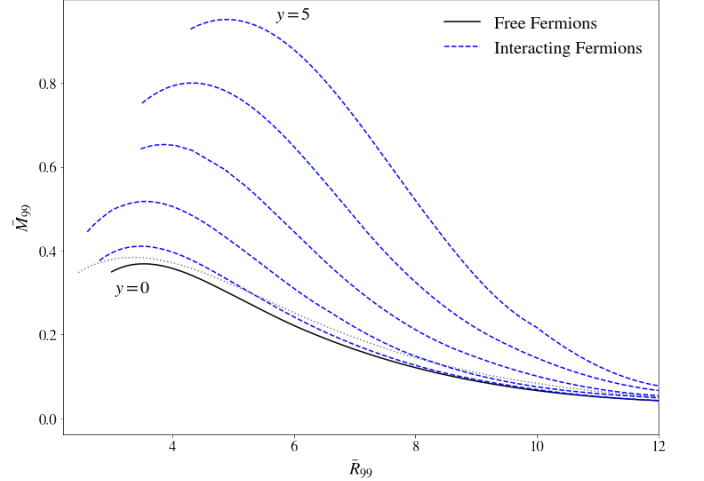


FIG. 4: As in Fig. 2, we obtained CDS configurations, but now in a R-square gravity with $\bar{\alpha} = 0.05$. Black solid line correspond to $y = 0$ and the blues dotted-lines corresponds to the dark star made of self-interacting fermions with coupling constant between $y = 1$ and $y = 5$. Grey line correspond to CDS in GR with $y = 0$ in order to compare GR and R-square CDS configurations.

where $\beta = \frac{1}{2}\sqrt{3\alpha}$. Thus, the gravitational force is increased if $\beta > 0$, and consequently, a lower amount of mass is needed to compensate the pressure produced by the fermions. This reduction in the mass of the configuration can be seen in Fig. 4 where we have included in a grey solid line the corresponding CDS configurations for $y = 0$ in GR. The black solid line that corresponds to R-square gravity is always below the grey line, meaning that all CDS in R-square gravity are smaller than the GR case.

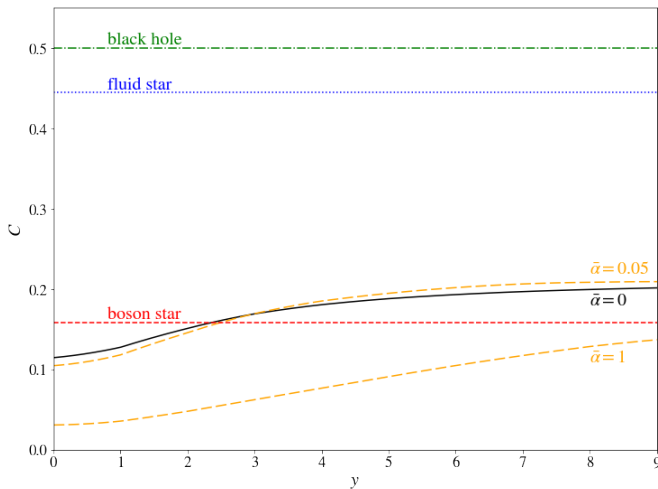


FIG. 5: Compactness of Fermionic dark stars as a function of the self-interaction strength parameter, y . The black solid line correspond to the case $\bar{\alpha} = 0$ (General Relativity), the orange dashes lines represent the compactness for two case, $\bar{\alpha} = 0.05$, and $\bar{\alpha} = 1$.

Another important observation is that the density tends to zero faster than the Ricci scalar, and then, the ADM-mass can increase even if the star has negligible contribution of fermions. The same holds for the derivative of the Ricci scalar. Thus, we can define a stellar radius r_s where the density is almost negligible $\rho(r_s) = 0$. Recall that we have the configuration radius r_* chosen by the shooting algorithm such as the boundary conditions are fulfilled. In general, $r_* > r_s$.

III. SIMILARITIES AND DIFFERENCES OF CDS IN GR AND R-SQUARE GRAVITY

A. Compactness

The Cold Dark Stars are objects made of self-interacting fermionic dark matter that do not interact with SM particles. For this reason they can not be observed by standard electromagnetic probes. However, in principle, they can be observed by gravity probes, such as gravitational wave (GW) signals or by the effect that CDS can induce gravitationally to other stars (e.g., [43, 44]). In the later case, an object that is far to the Cold Dark Star will feel the same gravitational potential both in GR and in R square gravity as long as the ratio M/R is the same. The parameter M/R is called the compactness of the star C defined as:

$$C = \frac{M_{ADM}}{R} = \frac{GM_{phys}}{R_{phys}c^2}, \quad (22)$$

where G is the gravitational constant and c the speed of light, and M_{phys} , R_{phys} are defined in eq. 13. Note that C is a dimensionless parameter. The compactness

of CDS is affected when we considered a self-interacting fermionic dark matter: the larger the value of y the bigger the mass, meanwhile the radius of the configuration is not severely affected by the value of y and thus, the compactness of the star increases as y increases. Changes in the compactness will imply changes in several properties such as the possible gravitational radiation emitted by an asymmetric star, or a binary of CDS and of course a change in the compactness induces changes in the gravitational potential the stars produce in other objects.

With this in mind, next we study the change in the maximum compactness of CDS as a function of the self-interacting strength constant y value. The compactness of the CDS in GR ($\bar{\alpha} = 0$) are shown as a solid black line in Fig. 5. In GR, for $y = 0$ (no self-interacting fermions) the maximum compactness is $C = 0.11$, and it increases as y increases. To have an order of magnitude, let us recall that the Sun compactness is $\sim 10^{-5}$. Thus CDS can be very compact objects. As a comparison of other compact objects, in Fig. 5 we have included other important compactness values. For instance, the maximum compactness for a fluid star, which is given by the Buchdahl's limit and that is given by $C = 4/9$ [45] is shown as a blue dotted line. In addition, the compactness of a Schwarzschild black hole, i.e. $C = 1/2$, is shown as a green dashed line. Finally, the maximum compactness for a Boson Star which is given by $C = 0.158$ [46] is plotted as a red dotted line. In summary: Fermionic CDS have a maximum stable compactness bigger than Boson Stars.

Now we can study Cold Dark Stars compactness in R-square gravity. It is important to recall that in R-square gravity one can distinguish between the asymptotic compactness $C = M_{ADM}/r_*$ - which captures contributions to the mass due to the non-vanishing value of the Ricci scalar. Nevertheless, r_* is formally reached at infinity as in the case of Boson Stars, because the Ricci scalar decays as $\sim 1/r^2$ and thus $R = 0$ can be reached only as $r_* \rightarrow \infty$. We used instead of the asymptotic compactness the following definition of compactness:

$$C = \frac{M_{99}}{R_{99}}, \quad (23)$$

where $M_{99} = 0.99M_{ADM}$ and R_{99} is the radius where M_{99} is reached.

We have plotted the maximum stable compactness (eq. 23) in R-square gravity as a function of the self-interacting coupling y in orange dashed lines of Fig. 5. Two values of $\bar{\alpha}$ were chosen: $\bar{\alpha} = 0.05$ and $\bar{\alpha} = 1$. For increasing values of $\bar{\alpha}$, the maximum compactness is decreasing, because the maximum mass in R-square gravity decreases meanwhile R_{99} is not severely affected. Note that there are configurations where the compactness for CDS in GR intersects the compactness for CDS in R-square gravity for different values of y . This intersection leads us to the confusion between dark matter properties with modifications of GR as we discuss in the next section.

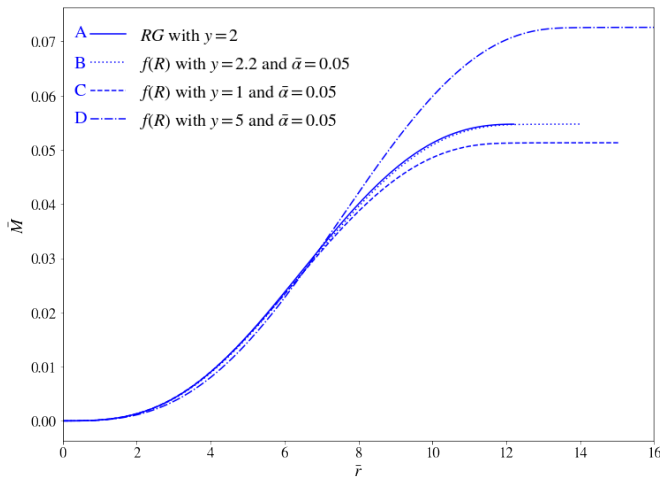


FIG. 6: For every case the mass profiles correspond to $f(R)$ theory are down to the mass profile obtained for the same case (same “ y ” value) but, using General Relativity. Is possible increase the mass obtained in R-squared in comparative we GR, if we choose for the first a higher value of “ y ”.

B. Confusing

The previous results show the linear relationship between the free parameter, y , α and the mass of the resulting CDS. In this section we will show that for a different selection of parameters m , y , α and $\bar{\rho}_0$ there are equivalent configurations, and thus, a confusing on the determination of the parameters is possible.

To illustrate this point, we have constructed three different configurations shown in Fig. 6:

- Configuration A: Solid line corresponds to $\bar{\rho}_0 = 4.1 \times 10^{-5}$, $y = 2$ (with self-interaction) $\bar{\alpha} = 0$ (General Relativity)
- Configuration B: Dotted line corresponds to $\bar{\rho}_0 = 4.1 \times 10^{-5}$, $y = 2.2$ (with self-interaction) $\bar{\alpha} = 0.05$ (R-square gravity)
- Configuration C: Dotted line corresponds to $\bar{\rho}_0 = 4.1 \times 10^{-5}$, $y = 1$ (with self-interaction) $\bar{\alpha} = 0.05$ (R-square gravity)
- Configuration D: Dashed line corresponds to $\bar{\rho}_0 = 3.4 \times 10^{-5}$, $y = 5$ (with self-interaction) $\bar{\alpha} = 0.05$ (R-square gravity)

Note that configuration B has the same central density as configuration A, but different interaction strength in R-square gravity. Nevertheless, the mass of the configuration and the radius are almost indistinguishable. Thus, any test particle will follow the same trajectory in both configurations.

On the other hand, Configuration C has a smaller central density, but due to the increase of the interaction strength y the total mass increases and it is above the

RG value. Thus, it seems that there will be a value of $\rho_0 \in [3, 4] \times 10^{-5}$ and $y \in [1, 5]$ for a R-square gravity with $\bar{\alpha} = 0.05$ will coincide with the GR case for $y = 2$ and $\bar{\rho}_0 = 4.1 \times 10^{-5}$. Thus any gravitational signal for this two objects will be almost identical for different values of the coupling constant.

There are other possible confusing possibilities in the determination of the parameters. Let us for instance construct all configurations with $y = 3$ in GR and all configurations for $y = 0$ in R-square gravity with $\bar{\alpha} = 0.05$. The plots M_{99} vs R_{99} for those configurations are shown in left panel of Fig. 7. Note that there are 2 points that intersect both plots. Those configurations corresponds to CDS with the same compactness. Thus, any other object will feel the same gravitational potential outside this CDS: no dynamical differences will be seen neither infall differences. Thus, if one luminous star is orbiting this cold Dark Star and this is the only observable we have to constraints the dark matter particle properties (remember that in this case that will be the mass of the dark matter particle and the self-interaction strength).

Finally, given the typical astrophysical uncertainties, small variations on the compactness or the M_{99} vs R_{99} relation will be difficult to be disentangled. On the top of that, we can have the already discussed confusing between GR and R-square gravity. Let us illustrate this final possibility by constructing all possible configurations with $y = 0.5$ in GR and all configurations for $y = 0$ in R-square gravity with $\bar{\alpha} = 0.1$. The plots M_{99} vs R_{99} for those configurations are shown in right panel of Fig. 7. Note that in this case there is an almost identical region where both plots intersect, and thus a infinite number of configurations can be confused.

IV. CONCLUSIONS

Modifications to general Relativity have been usually invoked to replace the role of dark matter or dark energy. Nevertheless, it could be possible that even with the existence of dark matter, there are possible modifications to general relativity. This modifications to GR seems to be mandatory specially if one looks for renormalizability of the gravitational interactions at high energies. Thus, we have consider a scenario where both dark matter and modifications to GR are present. In particular, we have consider dark matter as a self-interacting fermion in the degenerate limit and R-square gravity as a possible modification of GR. In this scenario, we have constructed self-gravitating structures made of this fermionic dark matter in both theories of gravity and studied their properties such as the compactness of the configurations. We have called this configurations Cold Dark Stars.

In the context of GR, we have shown that is possible to obtain configurations of CDS more compact than Boson Stars. Depending on the election of the mass of the fermion, CDS can be as massive and compact to be considered as black hole mimickers.

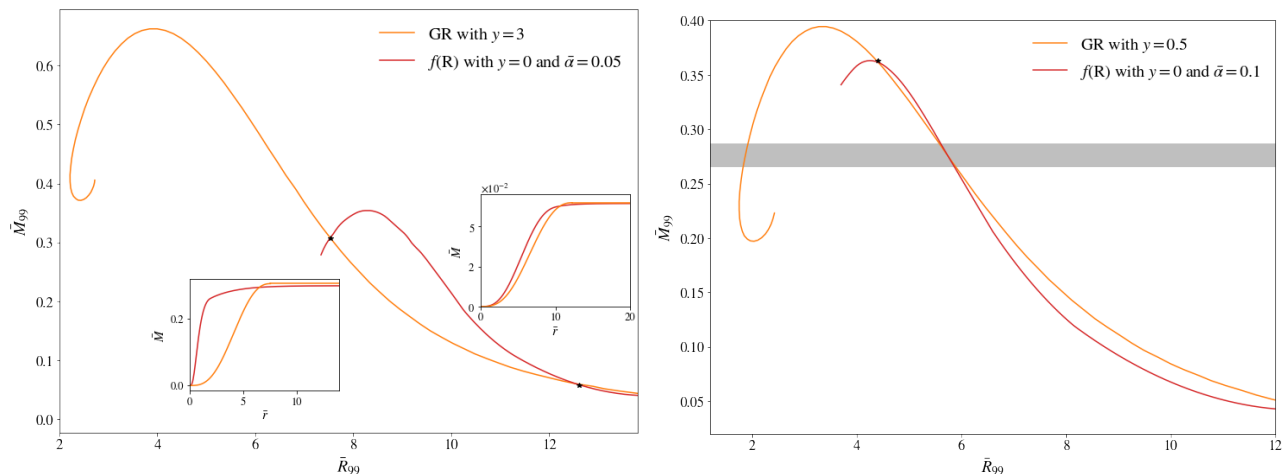


FIG. 7: The figures show the relationship between mass and radius in GR and $f(R)$. Left: The orange line correspond to all configurations (in the space parameter study) with GR and $y = 1$. The red line represent the same, but in $f(R)$ with $y = 0$. As see, exist confusing for some configurations (black points). This objects are indistinguishable one of other, because the have the same mass and radius. Right: Is illustrated the same idea, but whit other values for y and α . Now given the typical astrophysical uncertainties, small variations on the compactness will be difficult to be disentangled, the GR and $f(R)$. Note that in this case there is an almost identical region (dark region) where both plots intersects, and thus a infinite number of configurations can be confused

We have shown that CDS in R-square gravity, the bigger the quadratic term in the Einstein-Hilbert action, i.e. the bigger the value of $\bar{\alpha}$, the smaller the maximum mass of the resulting CDS configurations are obtained. This reduction in the mass will produce less compact CDS in R-square gravity in comparison with GR.

Considering the possibility that dark matter might interact only through gravitational interactions, the determination of their properties will be only accessible by astrophysical observations. Thus, given that similar CDS can be obtained for different election of coupling constants y or values of $\bar{\alpha}$ in R-square theories, thus, a possible confusion in the determination of the dark matter properties and possible modifications to general relativity

could be possible.

Acknowledgements

This work was partially support by CONACYT projects CB-259228 and CB- 286651 and Conacyt-SNI. We thank Alberto Diez-Tejedor and Gustavo Niz for very enlightening discussion regarding this work.

References

- [1] B. P. Abbott et al. Tests of General Relativity with GW170817. *Phys. Rev. Lett.*, 123(1):011102, 2019.
- [2] Jeremy Sakstein and Bhuvnesh Jain. Implications of the Neutron Star Merger GW170817 for Cosmological Scalar-Tensor Theories. *Phys. Rev. Lett.*, 119(25):251303, 2017.
- [3] Phillip James Edwin Peebles. Principles of physical cosmology. 1993.
- [4] Larson D. Weiland J. L. et al. Bennett, C. L. Nine-year Wilkinson Microwave Anisotropy Probe (WMAP) Observations: Final Maps and Results. *Astrophys. J.*, 208:54, 2013.
- [5] Daniel J. Eisenstein et al. Detection of the Baryon Acoustic Peak in the Large-Scale Correlation Function of SDSS Luminous Red Galaxies. *Astrophys. J.*, 633:560–574, 2005.
- [6] Shaun Cole et al. The 2dF Galaxy Redshift Survey: Power-spectrum analysis of the final dataset and cosmological implications. *Mon. Not. Roy. Astron. Soc.*, 362:505–534, 2005.
- [7] Shadab Alam et al. The clustering of galaxies in the completed SDSS-III Baryon Oscillation Spectroscopic Survey: cosmological analysis of the DR12 galaxy sample. *Mon. Not. Roy. Astron. Soc.*, 470(3):2617–2652, 2017.
- [8] Adam G. Riess et al. Observational evidence from supernovae for an accelerating universe and a cosmological constant. *Astron. J.*, 116:1009–1038, 1998.
- [9] D. M. Scolnic et al. The Complete Light-curve Sample of Spectroscopically Confirmed SNe Ia from Pan-STARRS1 and Cosmological Constraints from the Combined Pantheon Sample. *Astrophys. J.*, 859(2):101, 2018.
- [10] Y. Akrami et al. Planck 2018 results. I. Overview and the cosmological legacy of Planck. 2018.
- [11] Adam G. Riess, Stefano Casertano, Wenlong Yuan, Lucas M. Macri, and Dan Scolnic. Large Magellanic Cloud

- Cepheid Standards Provide a 1% Foundation for the Determination of the Hubble Constant and Stronger Evidence for Physics beyond Λ CDM. *Astrophys. J.*, 876(1):85, 2019.
- [12] Kenneth C. Wong et al. H0LiCOW XIII. A 2.4% measurement of H_0 from lensed quasars: 5.3σ tension between early and late-Universe probes. 2019.
- [13] Wendy L. Freedman et al. The Carnegie-Chicago Hubble Program. VIII. An Independent Determination of the Hubble Constant Based on the Tip of the Red Giant Branch. 2019.
- [14] Nils Schöneberg, Julien Lesgourgues, and Deanna C. Hooper. The BAO+BBN take on the Hubble tension. 2019.
- [15] C. Destri, H. J. de Vega, and N. G. Sanchez. Fermionic warm dark matter produces galaxy cores in the observed scales because of quantum mechanics. *New Astron.*, 22:39–50, 2013.
- [16] C. Destri, H. J. de Vega, and N. G. Sanchez. Quantum WDM fermions and gravitation determine the observed galaxy structures. *Astropart. Phys.*, 46:14–22, 2013.
- [17] Valerie Domcke and Alfredo Urbano. Dwarf spheroidal galaxies as degenerate gas of free fermions. *JCAP*, 1501(01):002, 2015.
- [18] Lisa Randall, Jakub Scholtz, and James Unwin. Cores in Dwarf Galaxies from Fermi Repulsion. *Mon. Not. Roy. Astron. Soc.*, 467(2):1515–1525, 2017.
- [19] J. Barranco, A. Bernal, and D. Delepine. Constraining ultra light fermionic dark matter with Milky Way observations. 2018.
- [20] Denys Savchenko and Anton Rudakovskiy. New mass bound on fermionic dark matter from a combined analysis of classical dSphs. *Mon. Not. Roy. Astron. Soc.*, 487(4):5711–5720, 2019.
- [21] L. Gabriel Gomez. Constraining light fermionic dark matter with binary pulsars. *Phys. Dark Univ.*, 26:100343, 2019.
- [22] M. Hanauske, L. M. Satarov, I. N. Mishustin, H. Stöcker, and W. Greiner. Strange quark stars within the nambu-jona-lasinio model. *Phys. Rev. D*, 64:043005, Jul 2001.
- [23] Alexei A. Starobinsky. A New Type of Isotropic Cosmological Models Without Singularity. *Phys. Lett.*, 91B:99–102, 1980. [771(1980)].
- [24] S. Gottlober, V. Muller, and Alexei A. Starobinsky. Analysis of inflation driven by a scalar field and a curvature squared term. *Phys. Rev.*, D43:2510–2520, 1991.
- [25] Jose A. R. Cembranos. Dark Matter from R2-gravity. *Phys. Rev. Lett.*, 102:141301, 2009.
- [26] Salvatore Capozziello and Mariafelicia De Laurentis. Extended Theories of Gravity. *Phys. Rept.*, 509:167–321, 2011.
- [27] Wayne Hu and Ignacy Sawicki. Models of $f(r)$ cosmic acceleration that evade solar system tests. *Phys. Rev. D*, 76:064004, Sep 2007.
- [28] Alexei A. Starobinsky. Disappearing cosmological constant in $f(R)$ gravity. *JETP Lett.*, 86:157–163, 2007.
- [29] Eric V. Linder. Exponential Gravity. *Phys. Rev.*, D80:123528, 2009.
- [30] Sergei D. Odintsov, Diego Sáez-Chillón Gómez, and German S. Sharov. Is exponential gravity a viable description for the whole cosmological history? *Eur. Phys. J.*, C77(12):862, 2017.
- [31] Gaurav Narain, Jurgen Schaffner-Bielich, and Igor N. Mishustin. Compact stars made of fermionic dark matter. *Phys. Rev.*, D74:063003, 2006.
- [32] Katherine Freese, Paolo Gondolo, J. A. Sellwood, and Douglas Spolyar. Dark Matter Densities during the Formation of the First Stars and in Dark Stars. *Astrophys. J.*, 693:1563–1569, 2009.
- [33] V. S. Berezhinsky, V. I. Dokuchaev, and Yu N. Eroshenko. Small-scale clumps of dark matter. *Phys. Usp.*, 57:1–36, 2014. [Usp. Fiz. Nauk184,3(2014)].
- [34] Katherine Freese, Tanja Rindler-Daller, Douglas Spolyar, and Monica Valluri. Dark Stars: A Review. *Rept. Prog. Phys.*, 79(6):066902, 2016.
- [35] L. D. Landau and E. M. Lifshitz. *Statistical Physics, Part 1*, volume 5 of *Course of Theoretical Physics*. Butterworth-Heinemann, Oxford, 1980.
- [36] David N. Spergel and Paul J. Steinhardt. Observational evidence for selfinteracting cold dark matter. *Phys. Rev. Lett.*, 84:3760–3763, 2000.
- [37] J D Barrow and A C Ottewill. The stability of general relativistic cosmological theory. *Journal of Physics A: Mathematical and General*, 16(12):2757–2776, aug 1983.
- [38] Artyom V Astashenok, Sergei D Odintsov, and Álvaro de la Cruz-Dombriz. The realistic models of relativistic stars in $f(r) = r + \alpha r^2$ gravity. *Classical and Quantum Gravity*, 34(20):205008, sep 2017.
- [39] Savaş Arapoğlu, Cemsinan Deliduman, and K. Yavuz Ekşi. Constraints on perturbative $f(r)$ gravity via neutron stars. *Journal of Cosmology and Astroparticle Physics*, 2011(07):020–020, jul 2011.
- [40] Joachim Näf and Philippe Jetzer. On the $1/c$ expansion of $f(r)$ gravity. *Phys. Rev. D*, 81:104003, May 2010.
- [41] W. T. Wetterling W. H. Press, S. A. Teukolsky and B. P. Flannery. *Numerical Recipes in C. The Art of Scientific Computing*. Cambridge University Press; 2 edition, October 30, 1992.
- [42] K. S. Stelle. Classical Gravity with Higher Derivatives. *Gen. Rel. Grav.*, 9:353–371, 1978.
- [43] Carlos Palenzuela, Paolo Pani, Miguel Bezares, Vitor Cardoso, Luis Lehner, and Steven Liebling. Gravitational Wave Signatures of Highly Compact Boson Star Binaries. *Phys. Rev.*, D96(10):104058, 2017.
- [44] Miguel Bezares and Carlos Palenzuela. Gravitational Waves from Dark Boson Star binary mergers. 2018.
- [45] H. A. Buchdahl. General relativistic fluid spheres. *Phys. Rev.*, 116:1027–1034, Nov 1959.
- [46] Pau ”Amaro-Seoane, Juan Barranco, Argelia Bernal, and Luciano” Rezzolla. ”Constraining scalar fields with stellar kinematics and collisional dark matter”. ”*JCAP*”, ”1011” : ”002”, ”2010”.